Sureshkumar et al. 2014. *Int. J. Vehicle Structures & Systems*, 6(4), 88-92
ISSN: 0975-3060 (Print), 0975-3540 (Online)
doi: 10.4273/ijvss.6.4.01

International Journal of Vehicle Structures & Systems
Available online at www.maftree.org/eja

Finite Element Simulation of Ballistic Performance of Dissimilar Metallic Plates Welded Joints

S. Sureshkumar[a], K. Sushinder[b] and S. Sudersan[c]

Dept. of Mechanical Engg., SSN College of Engineering, Chennai, India.
[a]Corresponding Author, Email: sureshkumars@ssn.edu.in
[b]Email: sushinder12109@mech.ssn.edu.in
[c]Email: sudersan12106@mech.ssn.edu.in

ABSTRACT:

Studies of ballistic penetration into metal plates and their numerical simulation currently play a vital role in the defence sector. However, no congruent results have been presented so far, especially when it comes to impact on welded plates. Furthermore, these issues are investigated for normal impacts and very few have made an attempt for oblique impacts. Thus the aim of the present work is to conduct numerical simulation using Abaqus/Explicit in order to evaluate the ballistic performance of similar and dissimilar welded plates subjected to various bullet velocities and impact angles. The effect of post weld residual stresses and associated plastic damage on the ballistic performance of similar (Al6061) and dissimilar (Al 6061- SS 304) welded plates is also determined. The energy absorbed by the welded plates for various configurations was determined and the results are critically evaluated.

KEYWORDS:

Ballistic performance; Finite element simulation; Dissimilar welded joints; Residual stress; Oblique impact

CITATION:

S. Sureshkumar, K. Sushinder and S. Sudersan. 2014. Finite Element Simulation of Ballistic Performance of Dissimilar Metallic Plates Welded Joints, *Int. J. Vehicle Structures & Systems*, 6(4), 88-92. doi:10.4273/ijvss.6.4.01.

NOMENCLATURE AND ABBREVIATIONS:

SMAW	*Shield Metal Arc Welding*
EOS	*Equation of State*
FCUW	*Flux-Cored Arc Welding*
GTAW	*Gas Tungsten Arc Welding*
SEM	*Scanning Electron Microscope*
$\bar{\sigma}$	*Equivalent stress*
$\bar{\varepsilon}^{pl}$	*Equivalent plastic strain*
$\dot{\varepsilon}_0$	*Reference strain rate*
A	*Johnson-Cook initial yield stress*
B	*Johnson-Cook strain hardening coefficient*
C	*Johnson-Cook strain rate hardening coefficient*
n	*Strain hardening exponent*
m	*Thermal softening exponent*
θ_{tran}	*Transition temperature*
$\hat{\theta}$	*Current temperature*
θ_{melt}	*Melting temperature*
$\bar{\varepsilon}_f^{pl}$	*Strain at failure.*
p, q	*Mean stress and Von Mises stress respectively*
d_1 - d_5	*Johnson-Cook failure parameters*
ω	*Damage parameter*
ρ_0	*Initial density*
Γ_0	*Gruneisen coefficient*
c_0, s	*Parameters for EOS model*
r_b	*Surface heat flux radius*
Q	*Net heat input*
r	*Radial distance from the heat source centre*
$q(r)$	*Heat flux*
V, I	*Welding arc voltage and current respectively*
η	*Heat source efficiency*

1. Introduction

Ballistics is defined as the science dealing with a great variety of phenomena which occur from the moment an object is fired until its effects are observed in a target. Terminal ballistics deals with the effect of projectile on its target. The penetration of tank armour by armour - piercing ammunition is an important concern of terminal ballistics. The major cause of tank failure is due to impact loading caused by the bullet which penetrates through the tank sheet and causes tearing. Thus there is a need to determine the energy absorbing capability of the joints in the tank under various impact velocities. It is also important to determine the damage done to the target by the blast effect and flying fragments of shells. With nuclear weapons there is also damage from intense heat and radiation. The study of terminal ballistics helps scientists to develop more effective weapons and to devise means of defence against enemy weapons.

One of the main problems one has to face during the analysis of a bullet penetration regarding the physical mechanism of failure is strictly related to the shape of a projectile. Different types of bullets exhibit different penetration mechanisms, which consequently brings about diverse damage shapes. For instance, ogival bullets penetrate a target by a ductile hole growth mechanism, whereas blunt projectiles manifest a plug shear penetration mechanism. Some of the failure modes in impacted plates are shown in Fig. 1. Dissimilar welded joints have wide variety of applications in army tanks, aerospace ducting and nuclear piping components.

Undesirable residual stresses are caused by conventional welding process for metallic structures, where high tensile residual stress develops from a permanent misfit between the near weld region and the rest of the work piece. Residual stresses are self-equilibrating stresses that are present within a structure when no external force is applied. This tensile residual stresses cause the premature failure of the component, commonly via accelerated crack growth near the weld region. On the other hand introduction of compressive residual stresses can be beneficial in improving the fatigue life of a component by putting the work piece surface into compression and thus suppressing crack growth.

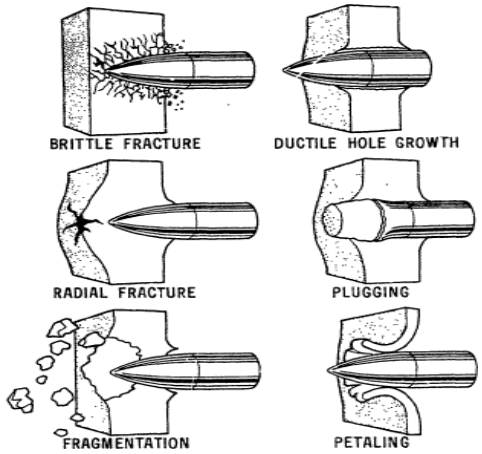

Fig. 1: Failure modes of impacted plates [1]

Flores-Johnson et al. [2] presented finite-element (FE) simulations that examine the effect of residual stress and associated plastic damage on the ballistic performance of welded austenitic steel plate. Reddy and Mohandas [3] experimentally studied the influence of welding process and residual stress on the ballistic impact performance of high-strength low-alloy ferrite steel plates which are welded by SMAW, FCAW and GTAW. It is observed that the ballistic performance of the heat affected zone improved in the case of SMAW when compared to FCAW and GTAW. Balakrishnan et al. [4] determined the effect of joint design on ballistic performance of armour grade quenched and tempered steel welded joints. Equal double 'V' and unequal double 'V' joint configurations were considered in their study. Of the two targets, the target made with unequal double 'V' joint configuration offered maximum resistance to the bullet penetration at weld metal region without any bulge at the rear side. Abhay et al. [5] conducted ballistic impact experiments for various impact velocities on AA2219 sheets using cylindrical ballistic projectiles which are made of hard steel.

The microstructure damage was analysed using SEM which consisted of adiabatic shear bands formed in extremely short time by the combined effects of the highly localized shear deformation and the high temperature rise that occurred in the shear bands. Amiri et al. [6] conducted numerical simulation of normal and oblique impacts on single and double-layered Al6061-T6 plates. It has been concluded that the ballistic limit is highest in single-layered plate. It has also been shown that the ballistic limit increases with increase in impact angle. Reported literature studies are limited to ballistic performance of similar welded joints. The objectives of the present work involving similar (Al6061) and dissimilar (Al 6061 - SS 304) welded plates are,

- To conduct FE simulation using Abaqus Explicit solver to evaluate the ballistic performance for various bullet velocities and impact angles.
- To determine the effect of post weld residual stresses and the associated plastic damage on the ballistic performance.
- To determine the impact energy absorbing capabilities of the welded plates for various weld configurations.

2. FE Simulation

Ballistic performance of plates for various impact velocities and bullet impinging angle was determined numerically. The target is Al6061-T6, 304mm square plate of thickness 26.3mm. The projectile is Steel 4340, 3.0 calliper radius head. The geometry and material properties of the target and projectile were considered from the literature [7]. Fig. 2 shows a schematic of the projectile.

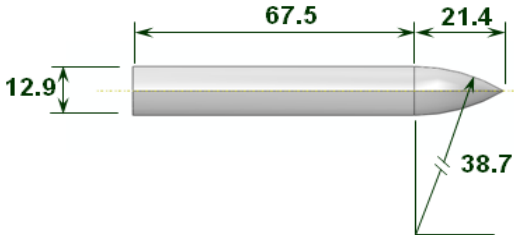

Fig. 2: Dimension of the ogive nosed projectile

2.1. Material Models

Johnson-Cook Plasticity' approach is used to account for strain rates, thermal effects and compressibility of plate material. The yield stress at non zero strain rate depends on the strain hardening, strain rate hardening and temperature softening such that,

$$\bar{\sigma} = \left(A + B\left(\bar{\varepsilon}^{pl}\right)^{n}\right)\left(1 + C\ln\left(\dot{\bar{\varepsilon}}^{pl}/\dot{\varepsilon}_0\right)\right)\left(1 - \hat{\theta}^{m}\right) \quad (1)$$

Where $\bar{\varepsilon}^{pl}$ is the equivalent plastic strain, $\dot{\varepsilon}_0$ is the reference strain rate. The parameters *A*, *B*, *C*, *n* and *m* are material parameters measured at or below the transition temperature θ_{tran}. $\hat{\theta}$ is the non-dimensional temperature which is equal to 1 when $\theta > \theta_{melt}$, 0 when $\theta < \theta_{tran}$, and is linearly proportional at temperature in-between. These parameters for the materials whose mechanical properties are close to the aluminium target and steel projectile are provided in Table 1.

Table 1: Parameters for Johnson-Cook plasticity model

Parameter	Target	Projectile
A (MPa)	262	1430
B (MPa)	162.1	2545
n	0.2783	0.7
θ_{melt} (K)	925	1793
θ_{tran} (K)	293.2	293.2
m	1.34	1.03
C	0	0.014
$\dot{\varepsilon}_0$ (1/s)	0	15.0

Johnson-Cook dynamic failure model' is used to define the mode of failure of the welded plates. This model is based on the damage parameter ω,

$$\omega = \sum \left(\Delta \bar{\varepsilon}^{pl} / \bar{\varepsilon}_f^{pl} \right) \quad (2)$$

Where $\Delta \bar{\varepsilon}^{pl}$ an increment of the equivalent plastic strain and $\bar{\varepsilon}_f^{pl}$ is the strain at failure.

$$\bar{\varepsilon}_f^{pl} = \left[d_1 + d_2 \exp\left(d_3 \frac{p}{q} \right) \right] \left[1 + d_4 1n \left(\frac{\dot{\bar{\varepsilon}}^{pl}}{\dot{\varepsilon}_0} \right) \right] \left(1 + d_5 \hat{\theta} \right) \quad (3)$$

Where p is mean stress, q is Von Mises stress, d_1-d_5 are failure parameters. Failure occurs when $\omega > 1$. Johnson-Cook failure parameters for aluminium target and steel projectile in the present analysis are given in Table 2.

Table 2: Parameters for Johnson-Cook dynamic failure model

Material	*d*1	*d*2	*d*3	*d*4	*d*5
Aluminium 6061-T6	-0.77	1.45	0.47	0.0	1.6
Steel 4340, Rc=38	0.05	3.44	2.12	0.002	0.61

Mie-Gruneisen equation of state (EOS) is used to model materials at higher pressure. This EOS model requires the input of the reference density ρ_0, Gruneisen coefficient Γ_0, parameters c_0 and s which define the linear relationship between the shock velocity and particle velocity. The values of these parameters used in the present analysis are given in Table 3.

Table 3: Parameters for Mie Gruneisen EOS model

Parameter	Al 6061-T6	Steel 4340, Rc=38
ρ_0 (g/cm^3)	2.703	7.83
Γ_0	1.97	1.67
c_0	0.524	0.4578
s	1.40	1.33
Ref. Temperature (K)	293.2	293.2
Specific heat (J/kg K)	885.0	477.0

Heat source modelling is used to capture exact temperature distribution and subsequently the weld induced imperfections. A heat source in welding is continuous travelling of spherical arc along the specified path on top surface of the work piece where fusion process is taking place. Distortion, residual stresses and reduced strength of structures result directly from the thermal cycle caused by localized intense heat input. The critical step in creating an efficient welding simulation strategy is to accurately compute the transient temperature distribution. Accurate modelling of moving heat source is mandatory in order to capture exact temperature distribution and subsequently the weld induced imperfections. The heat source is modelled by the following equation,

$$Q(r) = \left(3Q / \Pi r_b^2 \right) \exp\left(-3r^2 / r_b^2 \right) \quad (4)$$

Where r_b is surface heat flux radius. Q is the net heat input (W). r is the radial distance from the centre of the heat source and $q(r)$ is heat flux (W/m^2). The heat input is given by$Q = VI\eta$. The calculated heat input for FEA using V = 22V, I = 58A and η = 0.85 is 1084W. The temperature dependent material properties of Al6061 and SS309 for dissimilar welded plates are taken from [9].

2.2. FE Mesh Details

To start with, mesh convergence study was carried out to determine the optimum mesh size for the present problem. Around 9345 C3D8R hexahedral elements were used to build the model for aluminium plate and 2207 tetrahedral elements were used to build the model for projectile. Fig. 3 shows the plot of mesh size vs. Von Mises stress. Fine mesh of size 0.005 is done in the vicinity of the penetration zone based on mesh convergence studies. For similar and dissimilar welded plates 5490 C3D8T elements were used to build the model of the plate. Fig. 4 shows the meshed model of the welded plates and bullet. Contact interaction was defined between the plate and bullet tip. The contact region was partitioned from the base plate to apply fine mesh around the interface region.

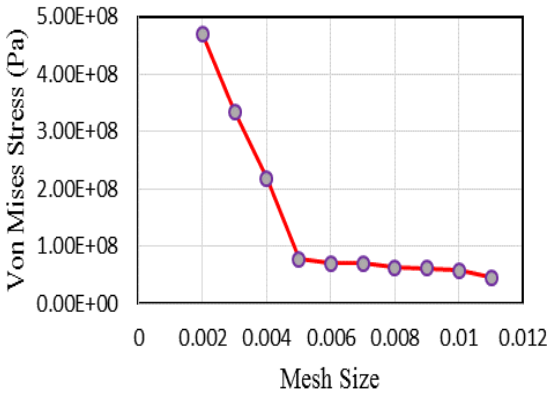

Fig. 3: Mesh convergence study

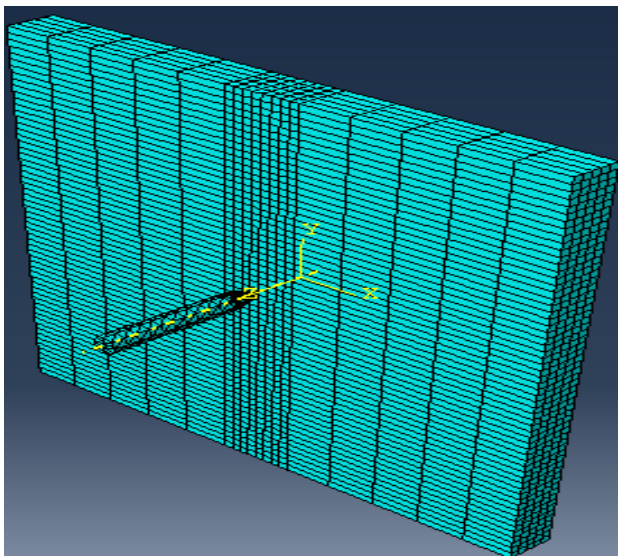

Fig. 4: FE mesh of welded bullet and projectile

2.3. Boundary Conditions

Conjugate heat transfer analysis was performed to determine the residual stresses induced. All four (right, left, top and bottom) sides of the plate are constrained in all degrees of freedom in step 1. In step 2, all four sides of the plates were locked in position and a surface heat flux of 9.16e6 (W/m^2) was applied over the weld region. Fig. 5 shows the boundary conditions applied on the FE model of welded plates.

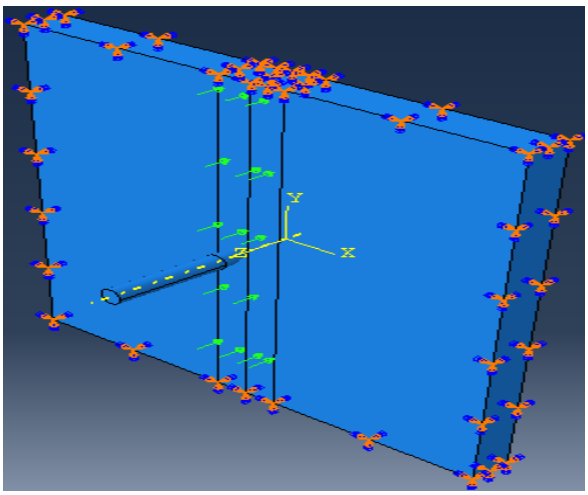

Fig. 5: FE model of weld plate with boundary conditions

3. Results and Discussions

3.1. Effect of Velocity

The ballistic performance of the plate geometry for various bullet velocities is plotted in Fig. 6. The ballistic performance is measured in terms of internal energy absorbed by the plate which increases with bullet velocity. Two different regions are noticed in the curve. It indicates the penetration of bullet through the plate. Fig. 7(a) and (b) shows the ballistic performance of similar and dissimilar welded joint subjected to various velocities respectively. The bullet was modelled in such a way that, to hit at the middle of the weld region. In this condition, the energy absorbed by the region increased for an increase in the bullet velocity. Higher energy absorption was noticed for dissimilar welded joint in comparison with similar welded joint.

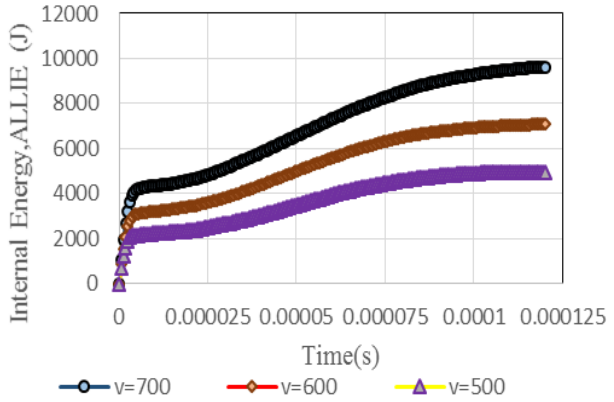

Fig. 6: Effect of bullet velocity on ballistic performance

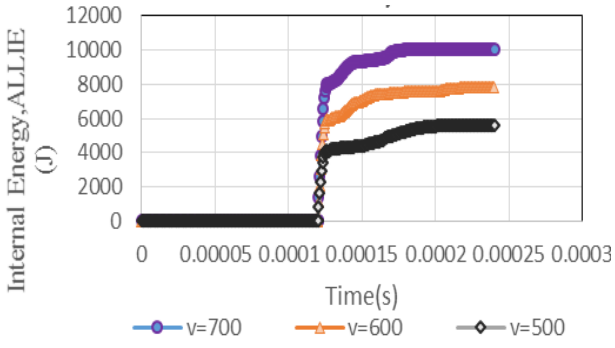

Fig. 7(a): Ballistic performance of similar welded joint

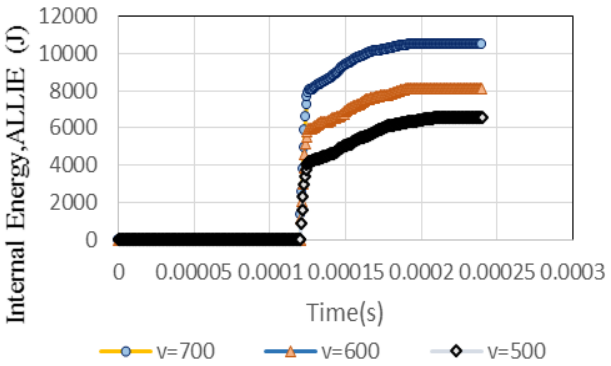

Fig. 7(b): Ballistic performance of dissimilar welded joint

3.2. Effect of Impact Angle

The ballistic performance of the plate geometry for various impact angles is plotted in Fig. 8. Fig. 9(a) and (b) shows the impact energy absorbing capability of similar and dissimilar welded plates respectively for various hitting angles which are varied from 22.5° to 90°. As the angle of impact increases, the internal strain energy of the plate decreases gradually. In the case of similar welded joints, highest impact energy was noted for a hitting direction of 90° to the plate. At lower angle of impact, energy absorbed by the plate is less as the bullet shears along the plate surface (see Fig. 10). In contrast to similar welded joint, higher impact energy is noted at lower angle in dissimilar welded joints. Irrespective of the joining process, the impact energy is constant at lower time steps. The failure mechanism of the dissimilar welded joint after the bullet hit is shown in Fig. 11. As the time step increases the bullet penetrates the plate and causes fragmentation type of failure.

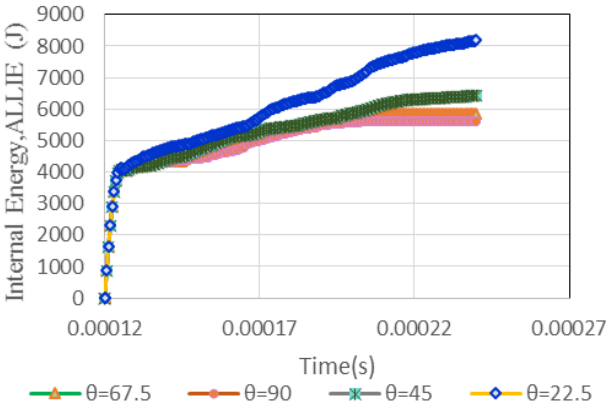

Fig. 8: Effect of impact angle on a single plate

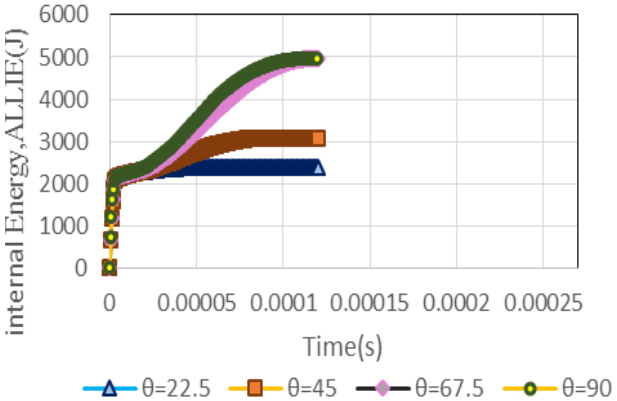

Fig. 9(a): Effect of impact angle on a similar welded joint

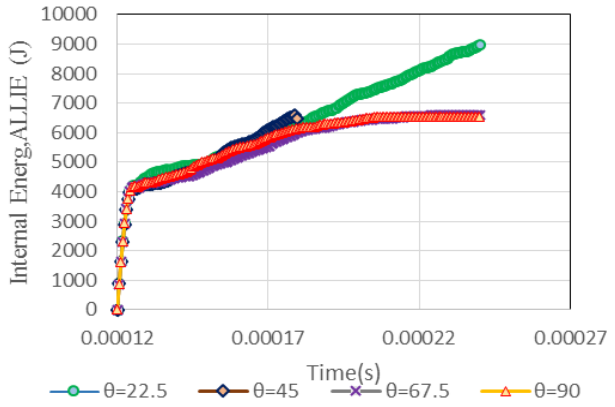

Fig. 9(b): Effect of impact angle on a dissimilar welded joint

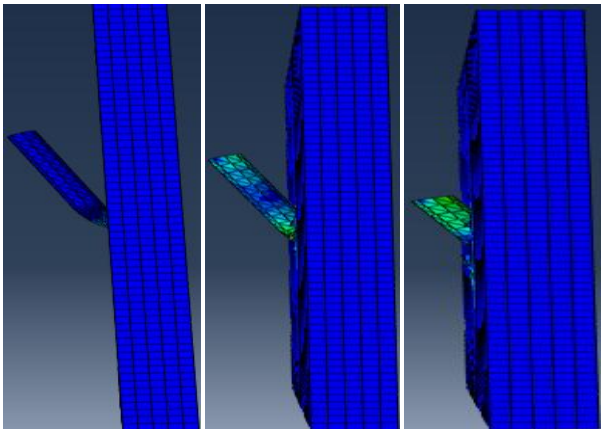

(a) At 0.0 μs (b) At 44.424 μs (c) At 125 μs

Fig. 10: Time scale representation of bullet impact on dissimilar welded plates at 22.5° impact angle

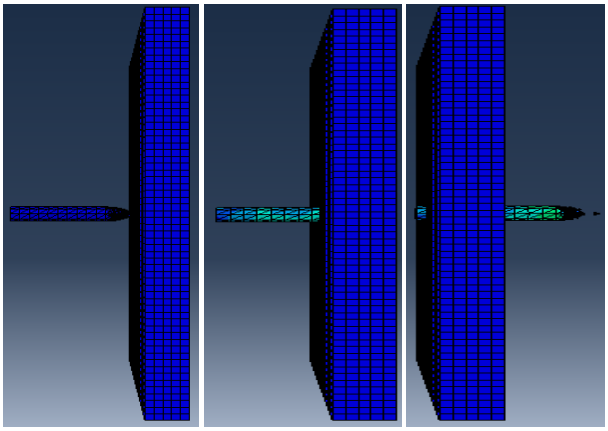

(a) At 0.0 s (b) At 36.046 μs (c) At 125 μs

Fig. 11: Time scale representation of bullet impact on dissimilar welded plates at 90° impact angle

4. Conclusions

Ballistic performance of similar and dissimilar welded joints has been determined numerically for various impact velocities and impact angles. As the bullet velocity increases, the internal energy of the plate also increases for both welded joints. A non linear variation of internal energy is observed due to plastic deformation. Internal energy of dissimilar welded joint was noted to be higher than similar welded joint irrespective of the considered bullet velocities. If the bullet is perpendicular to the target surface higher internal energy is observed and the value decreased for lower impact angles. The dominant mode of failure was observed to be fragmentation. As the initial bullet velocity increases, the internal energy of the target plate increased significantly. This effect is ratified by the absorption of bullet's kinetic energy by the target plate.

REFERENCES:

[1] J.A. Zukas. 1990. *High Velocity Impact Dynamics*, John Wiley & Sons.

[2] E.A. Flores-Johnson, O. Muránsky, C.J. Hamelin, P.J. Bendeich and L. Edwards. 2012. Numerical analysis of the effect of weld-induced residual stress and plastic damage on the ballistic performance of welded steel plate, *Computational Material Science*, 58, 131-139. http://dx.doi.org/10.1016/j.commatsci.2012.02.009.

[3] G.M. Reddy and T. Mohandas. 1996. Influence of welding process and residual stress on ballistic performance, *J. Mater. Sci. Lett*., 15, 1633-1635.

[4] M. Balakrishnanan, V. Balasubramanianan and G.M. Reddy. 2013. Effect of joint design on ballistic performance of quenched and tempered steel welded joints, *Materials and Design*, 54, 616-623. http://dx.doi.org/10.1016/j.matdes.2013.08.084.

[5] A.K. Jha, N. Siresha, S.V.S.N. Murthy, V. Diwakar and S. Kumar. 2005. Ballistic impact testing of AA2219 aluminium alloy welded plates and their metallurgical characterization, *Indian J. Engineering & Materials Sciences*, 12(3), 221-226.

[6] S. Amiri, M. Fossati, A. Gilioli, A. Manes and M. Giglio. 2012. Numerical simulations of normal and oblique impact on single and double-layered aluminium AL6061-T6 plates, Int. J. Engineering Modellig, 26(1-4), 37-43.

[7] Dassault Systèmes. 2012. Simulation of the ballistic perforation of aluminium plates with Abaqus/Explicit, *Abaqus Technology Brief*.

[8] M.P. Pandi and R. Kannan. 2014. Thermal analysis on butt welded aluminium alloy AA7075 plate using FEM, *Int. J. Engineering Research*, 3(2), 116-120.

[9] I.A. Khan. 2011. *Experimental and Numerical Investigation on the Friction Welding Process*, PhD Thesis, Faculty of Mech. Engg., Jawaharlal Nehru Technological University, India.

EDITORIAL NOTES:

Edited paper from International Conference on Advanced Design and Manufacture, 5-7 December 2014, Tiruchirappalli, Tamil Nadu, India.

GUEST EDITORS: Dr. T. Ramesh and Dr. N. Siva Shanmugam, Department of Mechanical Engineering, National Institute of Technology, Tiruchirappalli, Tamil Nadu, India.